The Journal of Chemical Physics

The effect of hydrogen bonds on the ultrafast relaxation dynamics of a BODIPY dimer

Cite as: J. Chem. Phys. **154**, 084201 (2021); https://doi.org/10.1063/5.0038242
Submitted: 20 November 2020 . Accepted: 31 January 2021 . Published Online: 23 February 2021

Elisa Fresch, Nicola Peruffo, Mariachiara Trapani, Massimiliano Cordaro, Giovanni Bella, Maria Angela Castriciano, and Elisabetta Collini

AIP Publishing

The Journal of Chemical Physics ARTICLE scitation.org/journal/jcp

The effect of hydrogen bonds on the ultrafast relaxation dynamics of a BODIPY dimer

Cite as: J. Chem. Phys. 154, 084201 (2021); doi: 10.1063/5.0038242
Submitted: 20 November 2020 • Accepted: 31 January 2021 •
Published Online: 23 February 2021

Elisa Fresch,[1] Nicola Peruffo,[1] Mariachiara Trapani,[2] Massimiliano Cordaro,[3] Giovanni Bella,[3] Maria Angela Castriciano,[2] and Elisabetta Collini[1,a)]

AFFILIATIONS

[1] Dipartimento di Scienze Chimiche, Università di Padova, via Marzolo 1, 35131 Padova, Italy

[2] CNR-ISMN, Istituto per lo Studio dei Materiali Nanostrutturati, c/o Dipartimento di Scienze Chimiche, Biologiche, Farmaceutiche ed Ambientali, V.le F. Stagno D'Alcontres 31, 98166 Messina, Italy

[3] Dipartimento di Scienze Chimiche, Biologiche, Farmaceutiche ed Ambientali, Università di Messina, V.le F. Stagno D'Alcontres 31, 98166 Messina, Italy

Note: This paper is part of the JCP Special Collection in Honor of Women in Chemical Physics and Physical Chemistry.
[a)] **Author to whom correspondence should be addressed:** elisabetta.collini@unipd.it

ABSTRACT

The influence of hydrogen bonds (H-bonds) in the structure, dynamics, and functionality of biological and artificial complex systems is the subject of intense investigation. In this broad context, particular attention has recently been focused on the ultrafast H-bond dependent dynamical properties in the electronic excited state because of their potentially dramatic consequences on the mechanism, dynamics, and efficiency of photochemical reactions and photophysical processes of crucial importance for life and technology. Excited-state H-bond dynamics generally occur on ultrafast time scales of hundreds of femtoseconds or less, making the characterization of associated mechanisms particularly challenging with conventional time-resolved techniques. Here, 2D electronic spectroscopy is exploited to shed light on this still largely unexplored dynamic mechanism. An H-bonded molecular dimer prepared by self-assembly of two boron-dipyrromethene dyes has been specifically designed and synthesized for this aim. The obtained results confirm that upon formation of H-bonds and the dimer, a new ultrafast relaxation channel is activated in the ultrafast dynamics, mediated by the vibrational motions of the hydrogen donor and acceptor groups. This relaxation channel also involves, beyond intra-molecular relaxations, an inter-molecular transfer process. This is particularly significant considering the long distance between the centers of mass of the two molecules. These findings suggest that the design of H-bonded structures is a particularly powerful tool to drive the ultrafast dynamics in complex materials.

I. INTRODUCTION

The role of hydrogen bonds (H-bonds) is central to understanding microscopic structures and functions in many functional biological and artificial materials. H-bonds stabilize and determine the 3D structure of biological macromolecules such as proteins and DNA and can play an essential role in determining the reactivity of the active site of enzymes.[1]

The directional nature of H-bonds has important implications not only for the final geometry of the complexes but also for their electronic properties. For example, it is known that in light-harvesting pigment–protein complexes, the establishment of specific and directional interactions tunes the site energies of the pigments.[2–4] We have also recently demonstrated that such interactions could have very strong consequences on the electronic coupling and the ultrafast dynamics of pigment–protein complexes.[5,6] These results suggested that it could be possible to tune the early time photophysics and the transport properties of multichromophores by engineering specific interactions with the surroundings and that H-bonds are particularly suited for this task because of the easiest control of orientations, distances, and geometries.

The physical and chemical properties of H-bonds in the ground state have been the subject of intense study.[7–9] H-bonds

dependent dynamical properties in the electronic excited state have also been widely investigated, although they remain more elusive. Upon photoexcitation of the H-bonded systems, the hydrogen donor and acceptor molecules reorganize due to the significant difference in the charge distribution of different electronic states. This reorganization process, which can lead to a weakening or a strengthening of the H-bond in the excited state with respect to the ground state,[10] has dramatic consequences on the mechanism, dynamics, and efficiency of photochemical reactions and photophysical processes of crucial importance for life and technology such as the photostability of RNA and DNA,[11,12] the photoinduced electron transfer reactions in biological photosynthesis,[13,14] and artificial photosynthesis and organic photovoltaics.[15–19] A thorough knowledge of these first ultrafast steps of the relaxation dynamics is therefore particularly urgent.

The electronic excited state H-bonding dynamics are predominantly determined by the vibrational motions of the hydrogen donor and acceptor groups and generally occur on ultrafast time scales of hundreds of femtoseconds. As a result, various femtosecond time-resolved spectroscopies have been used to unveil dynamics associated with transient H-bonding interactions taking place after the electronic excitation of the chromophores.[10,20,21] These techniques did not allow a time resolution better than 100 fs, and therefore, the details of the relaxation mechanisms at early times immediately after photoexcitation have not been fully clarified so far.[20]

To fill this gap, here, 2D electronic spectroscopy (2DES) is exploited. This technique is ideal for this aim since it conjugates superior time resolution (10 fs) with frequency resolution and sensitivity to the nuclear motion promoted by photoexcitation.[22,23] We performed 2DES measures on an H-bonded molecular dimer prepared by self-assembly of two boron-dipyrromethene (BODIPY) dyes driven by the formation of a triple H-bond (Fig. 1). The isolated monomer molecules have also been investigated in order to highlight the presence of ultrafast dynamic processes triggered by the establishment of H-bonds between the two monomeric units.

Numerous other examples in the literature described molecular complexes and materials with tailor-made designs involving H-bonded networks.[15,17,18,24–26] These structures have mainly been proposed to channelize photoinduced hydrogen or coupled electron–proton transfer reactions in artificial light-harvesting systems. Unlike this previous wealth of work, in this paper, we want to investigate the more fundamental issue of the influence of H-bonds on the ultrafast (sub-ps) dynamics. This aspect, still mostly unexplored, can substantially impact the design of future materials where H-bonds could be explicitly exploited to accelerate intermolecular energy dissipation or initiate and favor specific reaction channels.

II. RESULTS AND DISCUSSION

A. Design and preparation of the H-bonded dimer

BODIPY molecular moieties have been selected as the starting point for the preparation of the H-bonded dimer because of their well-known remarkable optical properties.[27–32] Here, distyryl-functionalized BODIPY has been considered to push their absorption spectrum in a spectral region convenient for the 2DES measurements (550 nm–750 nm). In previous works, we have already characterized by 2DES the mechanism and time scale of the femtosecond Stokes shift dynamics in analogous molecules[33] and investigated the role of specific solute–solvent interactions on their photophysical properties.[34]

In order to promote the formation of an H-bonded dimer, the donor and acceptor molecules were designed by introducing at the meso position of a distyryl-BODIPY moiety one-butyl-uracil (URA) and 2,6-diacetamido pyridine (DAAP) groups, respectively. The two molecules, denoted from now on as URA-BODIPY and DAAP-BODIPY, respectively, were prepared starting from the respective aldehydes used as precursors, as reported in Scheme 1.[35]

The dimer has been prepared by mixing equimolar concentrations of URA-BODIPY and DAAP-BODIPY in deuterated

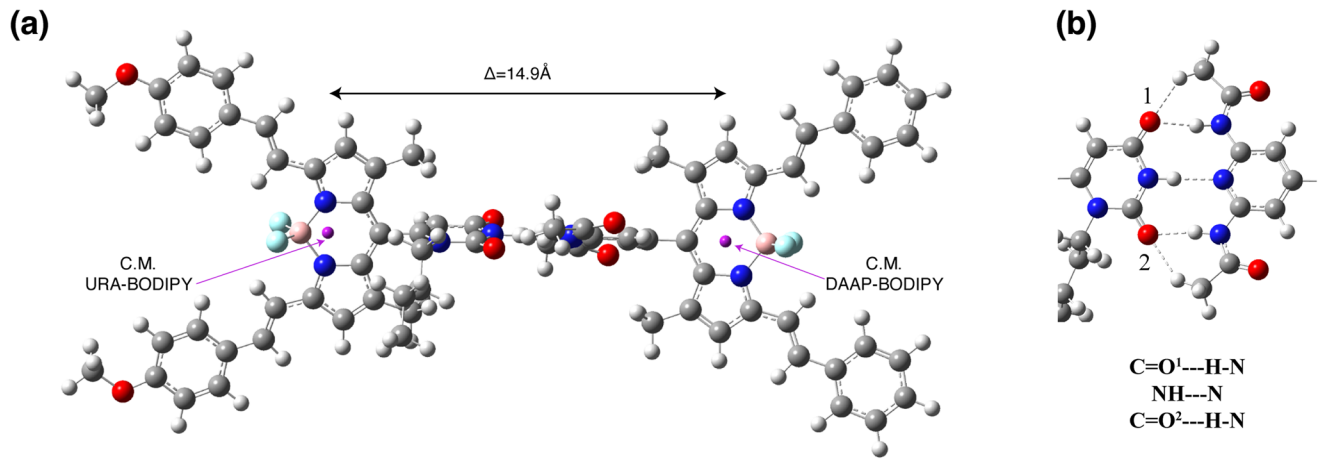

FIG. 1. (a) Association of the two chromophores as emerging from DFT calculations. The centers of mass (C.M.) of the two molecular units and their distance are pinpointed. (b) Zoomed-in view of the triple H-bond interaction. The role of the methyl groups of the DAAP in stabilizing the dimer formation is also highlighted.

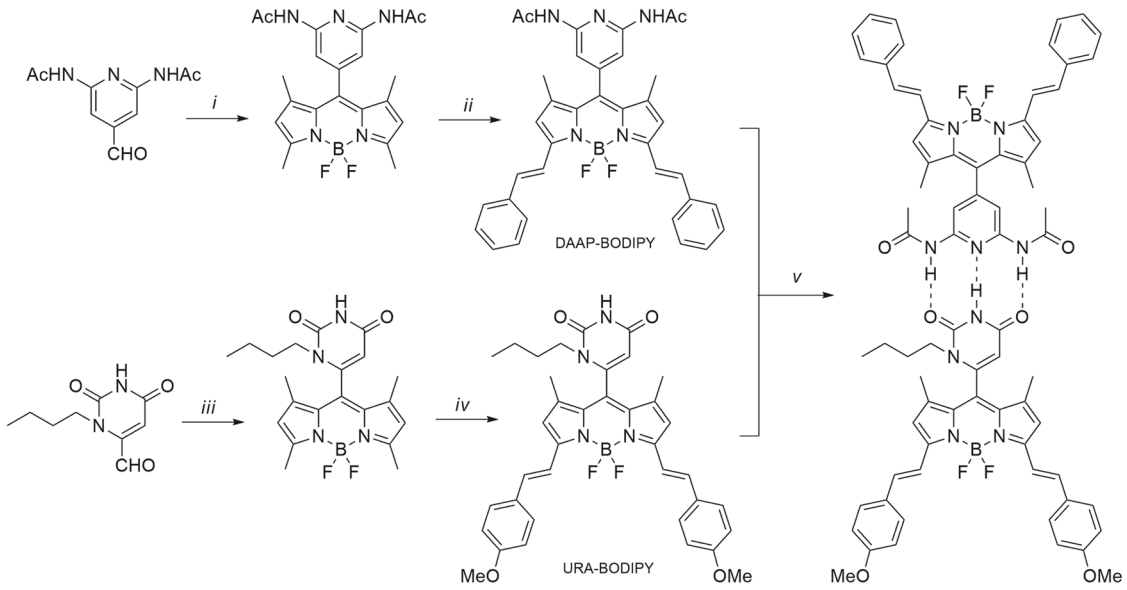

i: 1. 2,4-dimethylpyrrole, TFA; 2. p-chloranil; 3. Et_3N, BF_3-Et_2O
ii: PhCHO, piperidine, DMF
iii: 1. 2,4-dimethylpyrrole, TFA; 2. p-chloranil; 3. Et_3N, BF_3-Et_2O (one-pot)
iv: p-anisaldehyde, toluene, molecular sieves 5A in Dean-Stark
v: $CDCl_3$

SCHEME 1. The overall synthetic strategy of the DAAP-URA BODIPY dimer.

chloroform solutions. The dimer formation has been monitored and confirmed by ^{1}H NMR spectroscopy, following the changes in the chemical shift values of the hydrogen atoms involved in the H-bond formation (see the supplementary material).

Once it is verified that the dimer effectively forms in the solution, the structure and the electronic properties of the monomers and dimer have been preliminarily investigated through quantum mechanical calculations. The aim was to gain more insight into the geometry of the dimer and verify the presence of possible modifications in the structure and electronic proprieties promoted by the establishment of H-bonds. All the structures (URA-BODIPY, DAAP-BODIPY, and the dimer) were fully optimized (also verified by frequencies calculations) without symmetry constraints in the chloroform solvent employing the PCM method[36] using the *Gaussian09* package.[37] The conformational preferences of BODIPYs and their electronic properties were investigated by the CAM-B3LYP functional that combines B3LYP with the Coulomb-attenuating method.[38] The 6-311G (d,p) basis set was chosen as it represents a good compromise between accuracy and CPU time demand compared to the large size of our systems; two-electron integrals and their derivatives were calculated using an ultra-fine grid option. The results of the calculations on the single monomeric units are summarized in Figs. S2 and S3 of the supplementary material and confirm that, as expected, the H-bond promoting groups introduced at the meso positions are perpendicular to the BODIPY moiety and do not contribute significantly to the HOMO and LUMO orbitals of the molecules. The optimized association of the two chromophores by means of a triple H-bond interaction is reported in Fig. 1, where also the inter-chromophore distance (of about 1.5 nm) is estimated. At this inter-chromophore distance, we do not expect that a significant electronic coupling between the two monomers can be established. This is supported by the study of the frontier orbitals of the dimer (see Fig. S4 of the supplementary material) that reveals the absence of delocalization among the two moieties.

The results of simulations suggest that the complementarity in the self-assembly of the monomers is also assisted by methyl groups located on the DAAP scaffold [Fig. 1(b)].

B. Linear characterization

Figure 2 reports the linear absorption spectra measured for DAAP-BODIPY, URA-BODIPY, and the dimer dissolved in anhydrous chloroform ($CHCl_3$). The spectra of the two monomers exhibit the typical absorption bands of BODIPY chromophores.[28] The main absorption band at 632 nm (15 820 cm^{-1}) and 675 nm (14 810 cm^{-1}) for DAAP-BODIPY and URA-BODIPY, respectively, is assigned to the S_0–S_1 0-0 transition. The pronounced shoulders at higher energies can be instead identified with the vibronic progression composed of several vibrational states. The excitations to higher energy electronic states are usually less permitted and appear as weaker broad bands at shorter wavelengths.[28]

The absorption spectrum of the dimer is a combination of the spectra of the two monomers: it shows two prominent absorption bands at 631 nm (15 850 cm^{-1}) and 678 nm (14 750 cm^{-1}), slightly

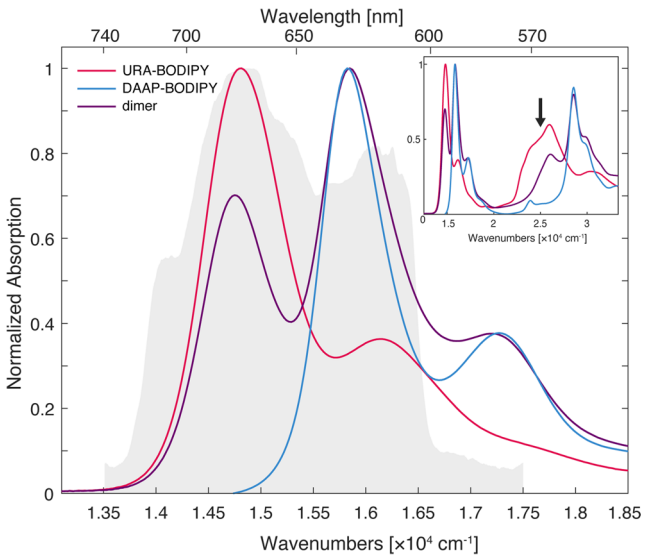

FIG. 2. Normalized absorption spectra of DAAP-BODIPY (blue), URA-BODIPY (red), and dimer (purple) in the 550 nm–750 nm spectral range. The gray area represents the laser spectrum profile used in the 2DES experiments. In the inset, the spectra in the whole visible range are reported and the arrow indicates the excitation wavelength in transient-absorption experiments.

shifted with respect to the ones of the two isolated monomers. These little spectral shifts may be attributed to the formation of the hydrogen bonds in the dimer, which is reported to have relatively small effects on the steady-state absorption spectra.[20]

Steady-state and time-resolved fluorescence of the building block monomers and the H-bonded dimer are reported in the supplementary material (Fig. S7 and Tables S1 and S2). In both cases, the response of the dimer appears as the sum of the separated molecular units. This behavior was expected based on the DFT calculations, indicating the absence of significant electronic coupling between the chromophores in the dimer. The fluorescence decay of the single monomeric units is mono-exponential with a lifetime value of 3.67 ns and 5.03 ns for the URA-BODIPY and DAAP-BODIPY, respectively. The emission decay of the dimer shows a biexponential behavior with a long lifetime value of about 5.26 ns (relative amplitude 30%) and a shorter one of about 3.47 ns (relative amplitude 70%) ascribable to the sum of the single units. Nonetheless, the anisotropy decay of the dimer shows a mono-exponential behavior with a rotational correlation time, which increases by about 0.4 ns with respect to the ones of the single monomers (Table S1). This represents additional evidence for the formation of a rotating unit larger than the isolated monomers.

C. Ultrafast dynamic characterization: Transient absorption spectroscopy

The ultrafast dynamics of the dimer and the two monomers have been preliminarily characterized by transient absorption (TA) spectroscopy, which allowed exploring the relaxation of the systems in the first nanosecond after photoexcitation with a time resolution of about 150 fs. The experiment has been performed pumping the system at 400 nm and using a white light supercontinuum (450 nm–700 nm) as probe light. More details about the experimental setup are reported in the supplementary material. The results are summarized in Fig. 3. Surprisingly, compared to the synthesis related manuscripts, there are only a few fs time-resolved photophysical studies on BODIPY dyes in the literature.[39–43]

Figures 3(a) and 3(b) show the TA spectra recorded at two selected values of the delay time for the three samples (more spectra in Fig. S7). For both monomeric species, the excitation at 400 nm results in the formation of negative ground state bleaching (GSB) features associated with the $S_0 \rightarrow S_1$ electronic transitions and the associate vibronic progressions (negative signals at 632 nm and 588 nm for DAAP-BODIPY and 675 nm and 625 nm for URA-BODIPY). Moreover, in both cases, at shorter wavelengths, a broad positive excited state absorption (ESA) signal ascribed to $S_1 \rightarrow S_n$ transition is recorded. These findings are in qualitative agreement with the TA spectra of other BODIPY dyes previously reported.[39–43]

The time dependence of the TA spectra of the monomers could be fitted with a bi-exponential kinetic model. The shortest time component (120 fs for URA-BODIPY and 160 fs for DAAP-BODIPY) is assigned to the formation of S_1 after relaxation from the higher energy state populated with the excitation at 400 nm ($S_{400} \rightarrow S_1$). The second time component has a time constant >1 ns, which could not be determined with better precision since it exceeds the investigated time window. This kinetics corresponds to the relaxation process from S_1 to the ground state S_0, in agreement with the time-resolved fluorescent lifetime measurements.

The TA spectrum of the dimer closely resembles the TA spectrum of the URA-BODIPY monomer. This is expected considering that at the excitation wavelength of 400 nm, the absorption spectrum of the dimer is dominated by the absorption features of the URA-BODIPY (see the inset in Fig. 2). Also in this case, the time evolution is described by a bi-exponential model with time constants of 140 fs and >1 ns. Although the values of these two time constants are very similar to the ones found for the monomeric species, the temporal response of the dimer cannot be explained as a mere sum of the behaviors of the two non-interacting chromophores. This is particularly evident in the 600 nm–640 nm region, as exemplified by the decay traces of the dimer and the URA-BODIPY monomer at 626 nm, reported in Figs. 3(c) and 3(d), respectively (more decay traces at different probe wavelengths in Fig. S9). In this spectral region, where there is a good overlap between the spectral features of the two monomers, the shortest ultrafast time component contributes to the overall relaxation dynamics as a decaying contribution in the dimer and as a growing contribution in the URA-BODIPY monomer.

These pieces of evidence seem to suggest that, at wavelengths where there is a good overlap between the spectral features of the two BODIPY moieties, a new dynamic process, not present in the isolated monomers, is activated upon dimer formation likely associated with a relaxation involving both URA- and DAAP-BODIPY moieties.

The overlap between the GSB features of two monomers, which sum up in the dimer, and the limited time resolution of the pump–probe technique make the assignment of the mechanism behind the relaxation dynamics of the dimer particularly challenging. 2DES

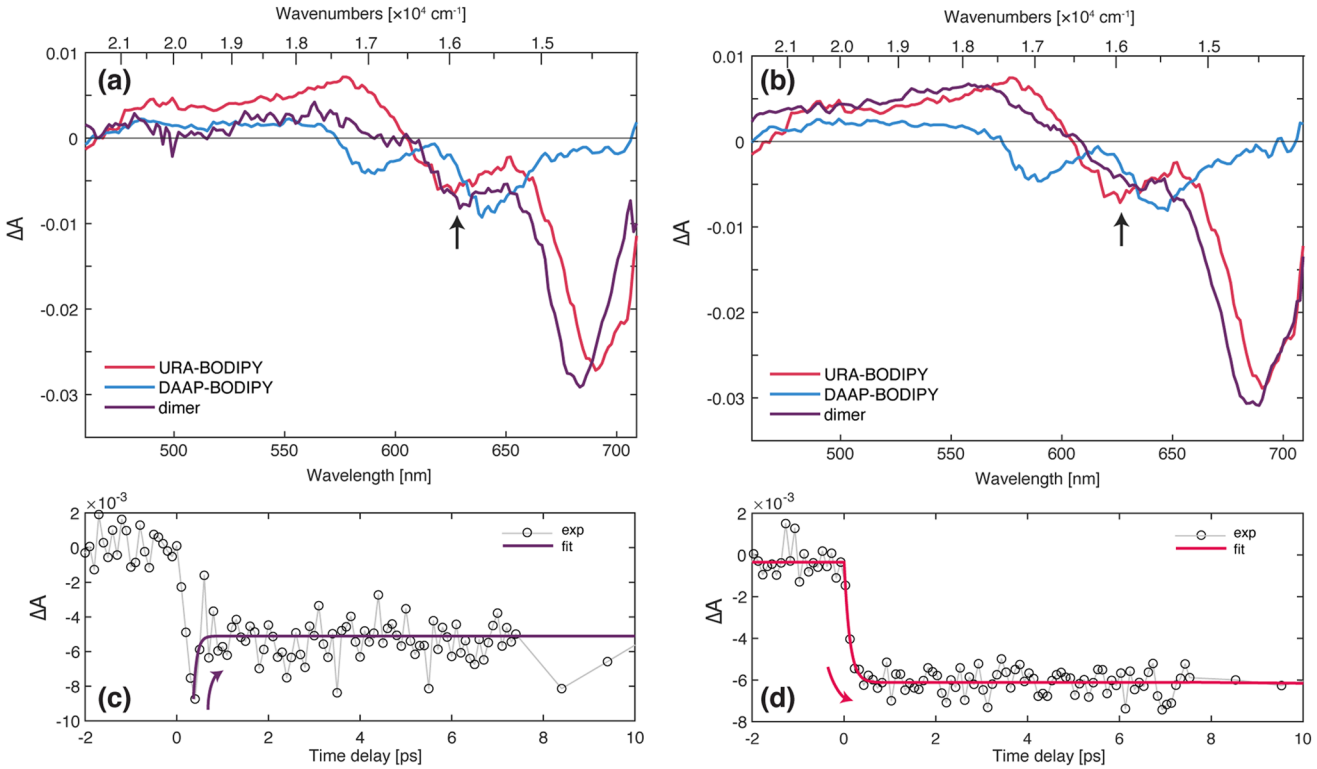

FIG. 3. (a) and (b) Transient absorption spectra (ΔA vs probe wavelength) for the three species at delay times equal to 0.5 ps (a) and 1 ps (b). [(c) and (d)] Decay traces (ΔA vs time delay) extracted at a probe wavelength of 626 nm [pinpointed by arrows in panels (a) and (b)] for the dimer (c) and URA-BODIPY monomer (d). The dots denote experimental points, while thick colored lines represent the result of the bi-exponential fitting. Curved colored arrows highlight the decaying (growing) contribution of the ultrafast time component in the dimer (URA-BODIPY; for additional data, see the supplementary material).

measurements have been exploited to help clarify these complex dynamics.

D. Ultrafast dynamic characterization: 2DES

For a better frequency and time characterization of the ultrafast relaxation in the dimer, we exploited 2DES, which allowed exploring a time window of 1 ps after photoexcitation, with a time resolution of about 10 fs. The 2DES signal is visualized in terms of 2D frequency–frequency maps correlating the excitation (x-axis) and emission (y-axis) frequencies for each value of the population time.[22,44,45] In this way, the 2DES technique, exploiting the Fourier transform methodology, can simultaneously provide frequency and time resolution.[23]

To compare the results of 2DES with the pump–probe ones, it is necessary to remember that the 2D spectrum is typically expressed in electric field units, contrary to TA spectra that are expressed in optical density units. This means that the signs of the 2D and pump–probe spectra are opposite. For example, the intense ground state bleaching of the URA-BODIPY monomer at 675 nm (14 810 cm^{-1}) appears as a negative feature in the TA spectrum of Figs. 3(a) and 3(b) and as a positive signal in the 2D spectra of Fig. 4(b). Also, TA spectra are typically reported as a function of the probe wavelength (in nm), while 2DES spectra are more often shown in energy units (eV or wavenumbers).

Figure 4 illustrates the evolution of the purely absorptive 2D spectra at selected values of population times for the three BODIPY species. For the DAAP-BODIPY [Fig. 4(a)], the exciting laser pulse overlaps with the 0-0 absorption band. The 2D maps show a positive diagonal peak, consistent with the position of the maximum of the absorption spectrum, originated by the ground-state bleaching (GSB) and stimulated emission (SE) of the S_1 state. In addition, two negative signals can be detected at symmetric upper and lower diagonal positions, interpreted as excited-state absorption (ESA) signals toward higher energy states, as already verified in the TA spectra.

At increasing values of population times, the initially diagonally elongated peak becomes more rounded and shifts to lower energies; in analogy with the previous literature,[46] after photoexcitation, the S_1 state relaxes as a result of intra- and intermolecular vibrational energy redistribution and solvent reorganization, resulting in a red shift of the stimulated emission (dynamic Stokes shift[47,48]). Simultaneously, the two negative signals progressively lose intensity; for the peak below the diagonal, this is also caused by the growth of the positive peak in the same spectral region, which compensates the negative ESA signal.

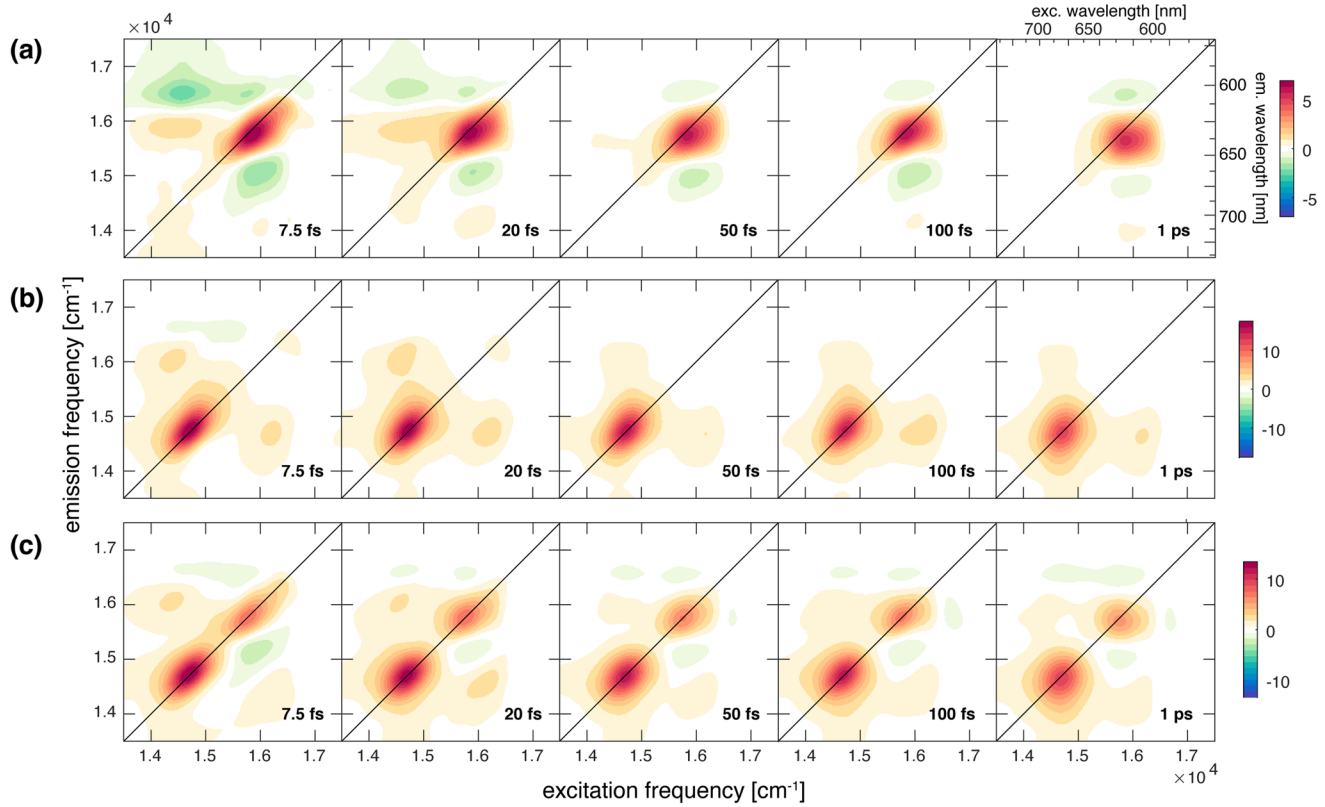

FIG. 4. Evolution of purely absorptive 2DES maps at selected values of the population time for (a) the DAAP-BODIPY monomer, (b) URA-BODIPY monomer, and (c) dimer. In the upper right map, the axes in wavelength units are also reported to ease the comparison with the results of TA spectroscopy.

The 2DES response of the URA-BODIPY [Fig. 4(b)] is qualitatively very similar to DAAP-BODIPY. Slight differences can be ascribed to the different overlap conditions between the absorption spectrum and the exciting laser profile, which, in this case, covers both the main absorption band and the vibronic shoulder. As for the DAAP-BODIPY monomer, the signal is dominated by a positive diagonal peak, attributed to the GSB and SE of the S_1 state, but there is no evidence of negative peaks in the regions above and below the diagonal. Nevertheless, in addition to the main diagonal peak, the presence of positive cross-peaks can be assessed at symmetric off-diagonal positions. These cross-peaks are typically associated with the excitation of vibrational modes, strongly coupled with the main transition.[45,49] As the population time increases, the signal, elongated at early times, evolves to a more circular shape and slightly red shifts, as for the DAAP-BODIPY monomer.

The 2D maps of the dimer [Fig. 4(c)] exhibit richer profiles as a result of the combination of the response of the two monomers composing the dimer. Qualitatively, the 2DES maps of the dimer appear as a sum of the responses of the two monomers.

To clarify the ultrafast dynamics and highlight possible differences between the behavior of the monomers and the dimer, the data have been analyzed through a global multi-exponential fitting procedure.[50] This global fitting methodology allows retrieving both the oscillating and non-oscillating dynamics of the 2DES response and could efficiently disentangle the different components that contribute to the evolution of the 2DES signal.[50]

Focusing first on the non-oscillating population dynamics of the two monomers, the global fitting reveals a bi-exponential decaying behavior, in agreement with what has been already reported in the literature.[33] The fitting results are shown in terms of 2D-DAS (2D-Decay Associated Spectra), where each spectrum of 2D-DAS represents the amplitude distribution of each time constant from the fitting as a function of excitation and emission frequency. For a positive signal, a positive (negative) amplitude in 2D-DAS means that the signal is exponentially decaying (rising) with the associated time constant.

For both DAAP-BODIPY and URA-BODIPY monomers, the fitting analysis revealed two time constants of about 15 fs and >1 ps. The associated 2D-DAS are reported in Fig. 5. The longer time constant (>1 ps) describes the overall decay dynamics to the ground state, which happens in times much longer than the investigated time window, as proved by pump–probe and time-resolved fluorescence experiments. For the DAAP-BODIPY monomer, these dynamics also includes the ESA signal above and below diagonal, whose intensity gradually decays with the same time constant.

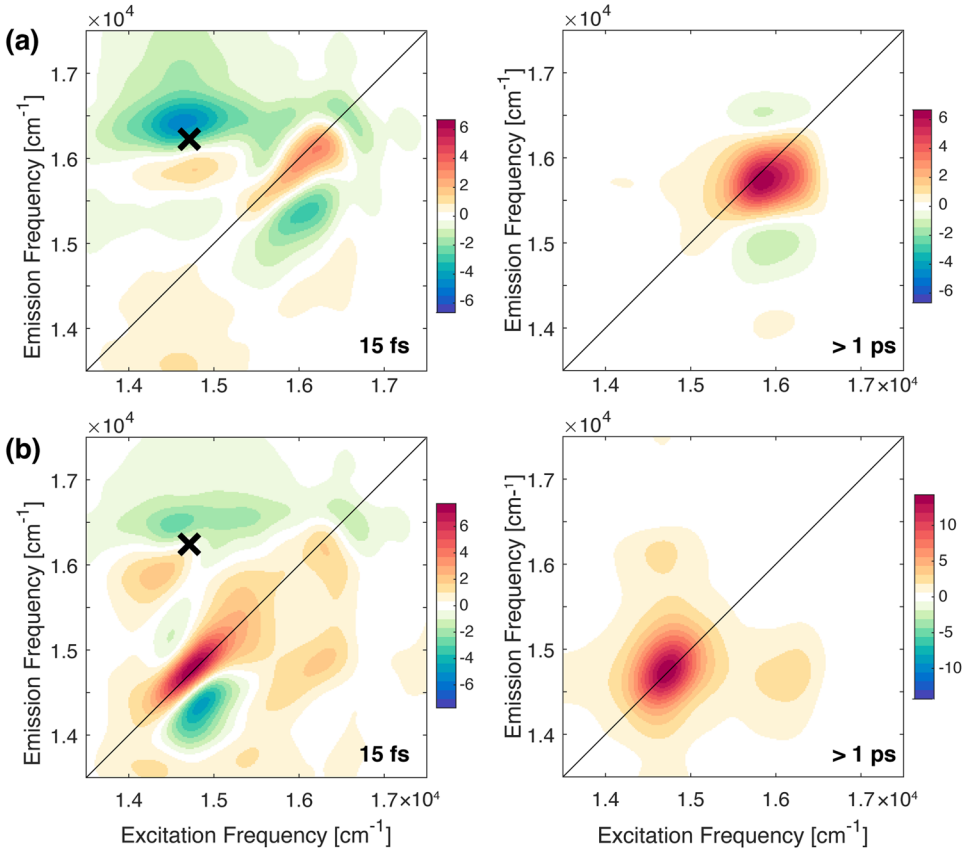

FIG. 5. 2D-decay associated spectra (2D-DAS) resulting from the global fitting of the 2DES maps for (a) DAAP-BODIPY and (b) URA-BODIPY monomers. The associated time constants are reported in each panel. The black cross marks the non-resonant contribution of the solvent at early times.

Regarding the shorter components, similar to what is already ascertained in previous measurements on BODIPY molecules with a similar structure, the decay can be interpreted as a combination of the spectral diffusion process[47] and the relaxation from the vertically excited Franck–Condon state toward a relaxed electronic configuration, mediated by solvent interactions.[33] In this ultrashort timescale, also the non-resonant contribution of the solvent appears in the upper diagonal portion of the DAS (black marker in Fig. 4). Clearly, this ultrashort time component could not be captured in the TA measures because of the limited time resolution. To conclude the comparison with the pump–probe results for the monomers, it should be noted that the 160 fs (120 fs) component, ascribed to the population of the S_1 state after excitation at 400 nm ($S_{400} \rightarrow S_1$) in DAAP-BODIPY (URA-BODIPY), could not be captured in the 2DES spectra because in this case, S_1 was directly excited (Fig. 2).

Figure 6 depicts the 2D-DAS resulting from the global fitting analysis of the dynamics of the dimer. Unlike the monomeric species, three components were necessary to fit the time behavior properly. The corresponding time constants are about 10 fs, 230 fs, and >1 ps.

The shortest and the longest time constants can be attributed to the same dynamic phenomena already examined for the monomeric species. More interesting is the 2D-DAS relative to the 230 fs time constant, which captures a dynamics absent in the non-interacting monomers. First, it should be noted that the presence of this additional ultrafast component has a time constant very similar to the one for the $S_{400} \rightarrow S_1$ process found in the TA spectra of the non-interacting monomers. This explains why in the TA spectrum of the dimer, these additional relaxation pathways could not be fully distinguished from the intra-chromophore $S_{400} \rightarrow S_1$ paths and just gave rise to a different signal amplitude contribution in the 600–640 spectral region [Fig. 3(c)].

Thanks to the intrinsic multidimensionality of the 2DES technique and the possibility of dispersing the amplitude associated with each time constant along two frequency dimensions in the 2D-DAS maps, the states effectively involved in this relaxation pathway can be clearly identified.[50]

The 2D-DAS for the 230 fs time component exhibits several signals. First, two positive signals appear in correspondence of the two main diagonal peaks concomitantly with two negative signals below the diagonal (pinpointed by squares in the second panel of Fig. 6); in analogy with the previous literature on different systems, such a signal distribution can be attributed to a downward relaxation within an excited state manifold.[5,33,51] It represents a relaxation channel that involves each of the two chromophores separately since we find the same behavior at (14 800, 14 800) and (15 800, 15 800) cm^{-1} diagonal coordinates, corresponding to the

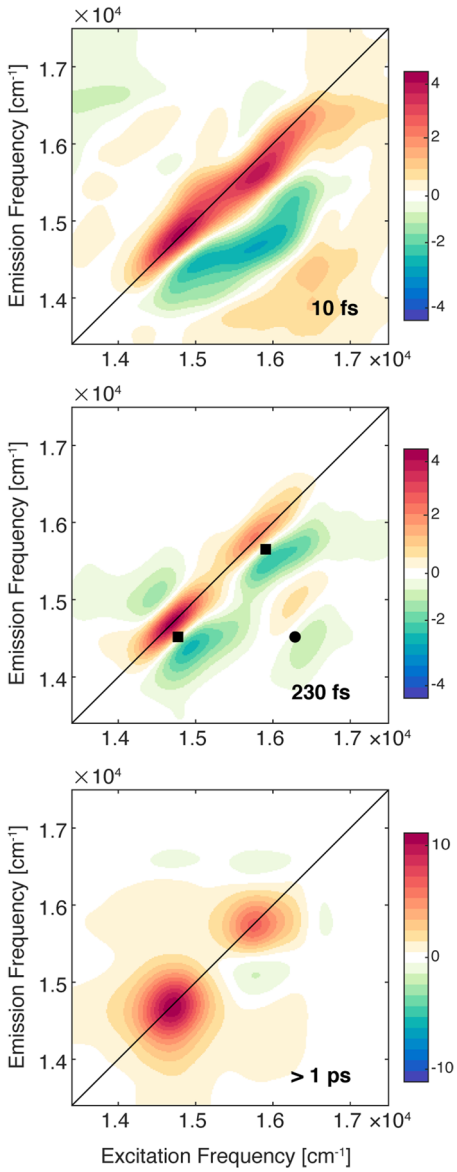

FIG. 6. 2D-decay associated spectra (2D-DAS) resulting from the global fitting of the 2DES maps for the dimer. The associated time constants are reported in each panel. Square and circle markers pinpoint relevant signals commented in the text.

energy of the S_1 state of the DAAP-BODIPY and URA-BODIPY monomers, respectively. Despite the intra-chromophore nature of the process, it is activated only when the two chromophores are coupled to form the dimer and shows the same dynamics for both chromophores.

In addition to that, a negative signal at cross-coordinates is distinguishable (circle). A negative signal at these coordinates means a transfer of population from a state at about 16 000 cm^{-1} (x-coordinate) to a state at 14 500 cm^{-1} (y-coordinate). This would suggest an inter-chromophore energy transfer from the S_1 of DAAP-BODIPY to the S_1 of URA-BODIPY with the same 230 fs dynamics.

Since both these intra- and inter-molecular relaxations are characterized by the same time constant, they likely share a common origin.

This inter-chromophore transfer cannot be attributed to a Förster energy transfer because of its ultrafast timescale. We can also exclude an excitonic mechanism promoted by a strong coupling between the two monomers, considering the significant inter-chromophore distance, the results of the DTF calculations, and the linear optical properties of the dimer.[52]

Previous work already demonstrated that H-bonded chromophores might reveal additional ultrafast dynamics associated with transient H-bonding interactions taking place after photoexcitation.[21] It was also established that these dynamics are promoted by a reorganization in the electronic excited state driven by H-bonding dynamics,[10] predominantly determined by the vibrational motions of the H donor and acceptor groups,[53,54] and generally occurring on time scales of hundreds of femtoseconds.[8,10,55,56]

In light of this, we speculate that the 230 fs dynamics, present in the dimer response but absent in the non-interacting monomers, could be attributed to a process involving intra and inter-chromophore relaxation phenomena, significantly coupled with the H-bond dynamics.

This assignment is also supported by the analysis of the beating dynamics. The presence of beatings in the signal amplitude as a function of the population time is a clear signature of coherent dynamics, i.e., of the time evolution of coherent superpositions of states prepared by the ultrafast laser excitation. These beatings can have different origins depending on the nature (vibrational, electronic, or vibronic) of the states building the coherent superpositions.[57–59] For organic chromophores in solutions, they are mainly caused by the time evolution of the vibrational modes more strongly coupled with the electronic transition promoted by the laser excitation, as also verified in the case of the two monomers. For this reason, 2DES has been often exploited to investigate which particular nuclei motions are more strongly coupled with the electronic transitions and verify if they have any role in the ensuing relaxation or transport dynamics.[5,46,51,60–62]

Considering that the electronic excited state H-bonding dynamics are predominantly determined by the vibrational motions of the H donor and acceptor groups, it is expected that the analysis of the beating behavior of the 2DES signal at relevant coordinates can therefore support the previous attribution of the 230 fs kinetics to intra- and inter-chromophore relaxation processes mediated by H-bonds.

The oscillating coherent dynamics have been studied with the same global fitting methodology described above as well as through conventional Fourier analysis. For all the samples, the overall beating behavior, quantified by the power spectra in Fig. 7(a), is dominated by a strong non-resonant contribution of the chloroform vibrational modes (261 cm^{-1}, 363 cm^{-1}, 680 cm^{-1}, and 1220 cm^{-1}),[63] as already verified with other samples dissolved in the same solvent.[64]

It is, however, possible to recover additional beating components. For the URA-BODIPY monomer, we found significant oscillations at 1190 cm^{-1}, 1280 cm^{-1}, 1460 cm^{-1}, 1500 cm^{-1}, and

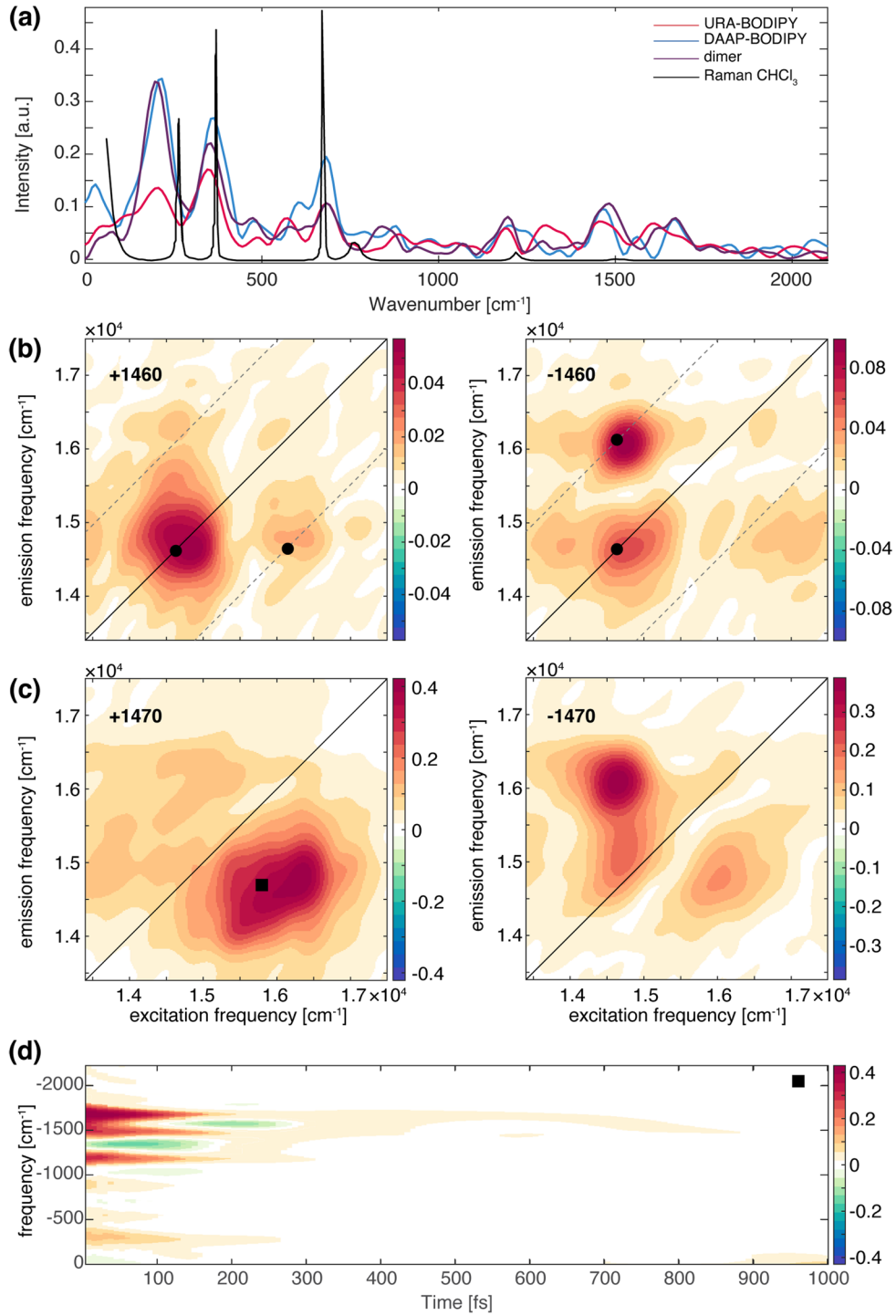

FIG. 7. Beating analysis of the 2DES signals. (a) Power Fourier spectra for the three species. Power spectra are obtained by Fourier transforming the 2DES maps along the population time t_2 after integration over the excitation and emission frequencies, and therefore, they capture the main components contributing to the overall beating behavior of the whole 2D maps. The Raman spectrum of the chloroform solvent is also reported for comparison (black line). (b) 2D-CAS obtained from the global fitting analysis of the URA-BODIPY monomer signal for a beating component with a frequency of ±1460 cm^{-1}. Analogous to 2D-DAS, the 2D-CAS show the amplitude distribution of a specific beating component in the 2D maps.[50] Black dots pinpoint coordinates where vibrational modes are expected to contribute. (c) Same as (b) but for the dimer. (d) Time-frequency transform[69,70] of the decay trace extracted at coordinates (16 000, 14 700) cm^{-1} corresponding to the square in panel (c).

1610 cm^{-1}. For the DAAP-BODIPY, additional components at 1190 cm^{-1}, 1253 cm^{-1}, 1470 cm^{-1}, and 1670 cm^{-1} were found in addition to the chloroform frequencies. In all cases, the amplitude distribution of these beating components in the 2D maps, plotted in the so-called 2D-CAS (coherent associated spectra),[50] presents the typical pattern predicted for vibrational modes.[5,49,59,65,66] Figure 7(b) exemplifies this analysis for the mode at 1460 cm^{-1} recorded for the URA-BODIPY monomer. The higher amplitude of the signal located above the diagonal (negative frequencies) suggests a stronger contribution of this mode in the excited state.[49,66] Also, the dynamic behavior of these beating modes supports their vibrational nature, presenting dephasing times in the order of ps.

The situation is different in the dimer case where three main components are found (1200 cm^{-1}, 1470 cm^{-1}, and 1660 cm^{-1}) with an amplitude distribution significantly different, as shown in Fig. 7(c) for the 1470 cm^{-1} frequency. These components contribute mainly to the 2DES signal below the diagonal at coordinates where the cross peak attributed to the 230 fs inter-molecular relaxation path is found.

All these modes can be attributed to vibrational modes involving functional groups and bonds implicated in the formation of H-bonds in the dimer. In particular, the frequencies at 1200 cm^{-1} and 1470 cm^{-1} are typically associated with vibrational modes of amino groups involving N–H bending and C–N stretching, while the mode at 1660 cm^{-1} is more strongly related to the C=O stretching.[67,68] Their dynamic behavior is also peculiar, being characterized by damping times of about 150 fs, as quantified by the global fitting and visualized through time-frequency transform (TFT) analysis [Fig. 7(d)].[69,70] Therefore, summarizing the properties of these beating modes: (i) they are most likely connected with functional groups involved in the H-bonds formation, (ii) they do not present the typical amplitude distribution expected for vibrational modes, but they contribute mainly at a cross-peak position where an inter-molecular transfer mechanism has been identified, and (iii) the beating dynamics associated with these modes are damped in the same timescale of this inter-molecular transfer process. All these pieces of information point toward the effective presence of an active mediating role of the H-bonds in the ultrafast dynamics of the dimer.

The envisioned mechanism provides that after photoexcitation of the H-bonded dimer, a reorganization of the charge distribution occurs. This reorganization involves both intra- and inter-molecular processes, and it is driven by the vibrational motions of the H donor and acceptor groups.

III. CONCLUSIONS

An H-bonded dimer of BODIPY chromophores has been designed and synthesized with the specific aim of verifying to what extent the presence of H-bonds could affect the ultrafast dynamic relaxation in the excited state.

Pump–probe and 2DES measurements, performed on both the monomeric units and the dimer, revealed that the formation of a dimer opens up a new ultrafast relaxation channel, characterized by a time constant of about 200 fs. The multidimensionality of the 2DES technique allowed analyzing the amplitude distribution of this time component as a function of the excitation and emission frequency and identifying the states involved in these dynamics. This analysis revealed the presence of two kinds of processes contributing to these dynamics.

First, we detected an "intra-molecular" relaxation pathway, which involves the two chromophoric moieties separately but simultaneously, i.e., with the same time constant. Second, an "inter-molecular" relaxation mechanism involves the transfer of population from the S_1 of DAAP-BODIPY to the S_1 of URA-BODIPY. The analysis of the beating behavior of the 2DES signals, mainly connected with nuclear motions, revealed the presence of peculiar features in the dimer, developing in a timescale of about 150 fs and attributable to vibrational motions of the groups involved in the H-bond.

In light of these pieces of evidence and comparing with the previous literature on excited-state H-bond dynamics, it is likely to conclude that the H-bonds activates new ultrafast dynamic channels in the relaxation dynamics of the dimer involving intra- and inter-molecular mechanisms.

The activation of an inter-molecular mechanism is particularly significant considering the very weak interaction of the two BODIPY molecules and the considerable distance between their centers of mass (about 1.5 nm). This indeed suggests that the design of H-bonded structures is a particularly powerful tool to drive the ultrafast dynamics in complex materials.

SUPPLEMENTARY MATERIAL

See the supplementary material for additional details on synthetic procedures, DFT simulations, and further experimental data.

DEDICATION

E.C. dedicates this work to Professor Camilla Ferrante, who pioneered ultrafast experiments in the Department of Chemical Sciences of Padova.

ACKNOWLEDGMENTS

This work was financially supported by MIUR PRIN 2017 under Grant No. 2017A4XRCA. The authors also acknowledge the support of MIUR PRIN 2015 under Grant No. 2015XBZ5YA. E.F. acknowledges a Ph.D. fellowship from the Department of Excellence program "NExuS."

The authors declare no conflict of interest.

DATA AVAILABILITY

The data that support the findings of this study are available from the corresponding author upon reasonable request.

REFERENCES

[1]G. A. Jeffrey and W. Saenger, *Hydrogen Bonding in Biological Structures* (Springer, Berlin, 1991).

[2]M. J. Llansola-Portoles, F. Li, P. Xu, S. Streckaite, C. Ilioaia, C. Yang, A. Gall, A. A. Pascal, R. Croce, and B. Robert, Biochim. Biophys. Acta, Bioenerg. **1861**, 148078 (2019).

[3]K. McLuskey, S. M. Prince, R. J. Cogdell, and N. W. Isaacs, Biochemistry **40**, 8783 (2001).
[4]J. N. Sturgis and B. Robert, J. Phys. Chem. B **101**, 7227 (1997).
[5]E. Fresch, E. Meneghin, A. Agostini, H. Paulsen, D. Carbonera, and E. Collini, J. Phys. Chem. Lett. **11**, 1059 (2020).
[6]A. Agostini, E. Meneghin, L. Gewehr, D. Pedron, D. M. Palm, D. Carbonera, H. Paulsen, E. Jaenicke, and E. Collini, Sci. Rep. **9**, 18255 (2019).
[7]T. Elsaesser, Acc. Chem. Res. **42**, 1220 (2009).
[8]E. T. J. Nibbering and T. Elsaesser, Chem. Rev. **104**, 1887 (2004).
[9]M. Banno, K. Ohta, S. Yamaguchi, S. Hirai, and K. Tominaga, Acc. Chem. Res. **42**, 1259 (2009).
[10]G.-J. Zhao and K.-L. Han, Acc. Chem. Res. **45**, 404 (2012).
[11]D. Tuna, A. L. Sobolewski, and W. Domcke, J. Phys. Chem. A **118**, 122 (2014).
[12]K. Kleinermanns, D. Nachtigallová, and M. S. de Vries, Int. Rev. Phys. Chem. **32**, 308 (2013).
[13]P. M. Krasilnikov, P. A. Mamonov, P. P. Knox, V. Z. Paschenko, and A. B. Rubin, Biochim. Biophys. Acta, Bioenerg. **1767**, 541 (2007).
[14]K.-H. Tang and R. E. Blankenship, in *Encyclopedia of Biophysics*, edited by G. C. K. Roberts (Springer Berlin Heidelberg, Berlin, Heidelberg, 2013), pp. 1868–1873.
[15]J. L. Sessler, M. Sathiosatham, C. T. Brown, T. A. Rhodes, and G. Wiederrecht, J. Am. Chem. Soc. **123**, 3655 (2001).
[16]J. Otsuki, J. Mater. Chem. A **6**, 6710 (2018).
[17]L. Sánchez, M. Sierra, N. Martín, A. J. Myles, T. J. Dale, J. Rebek, Jr., W. Seitz, and D. M. Guldi, Angew. Chem., Int. Ed. **45**, 4637 (2006).
[18]M.-L. Yu, S.-M. Wang, K. Feng, T. Khoury, M. J. Crossley, F. Yang, J.-P. Zhang, C.-H. Tung, and L.-Z. Wu, J. Phys. Chem. C **115**, 23634 (2011).
[19]A. Dey, J. Dana, S. Aute, A. Das, and H. N. Ghosh, Photochem. Photobiol. Sci. **18**, 2430 (2019).
[20]A. Swain, B. Cho, R. Gautam, C. J. Curtis, E. Tomat, and V. Huxter, J. Phys. Chem. B **123**, 5524 (2019).
[21]E. Pines, D. Pines, Y.-Z. Ma, and G. R. Fleming, ChemPhysChem **5**, 1315 (2004).
[22]A. M. Branczyk, D. B. Turner, and G. D. Scholes, Ann. Phys. **526**, 31 (2013).
[23]A. Gelzinis, R. Augulis, V. Butkus, B. Robert, and L. Valkunas, Biochim. Biophys. Acta, Bioenerg. **1860**, 271 (2019).
[24]X. He, F. Yang, S. Li, X. He, A. Yu, J. Chen, J. Xu, and J. Wang, J. Phys. Chem. A **123**, 6463 (2019).
[25]J. Bonin, C. Costentin, M. Robert, J.-M. Savéant, and C. Tard, Acc. Chem. Res. **45**, 372 (2012).
[26]B. Wang, R.-B. Lin, Z. Zhang, S. Xiang, and B. Chen, J. Am. Chem. Soc. **142**, 14399 (2020).
[27]R. Ziessel, G. Ulrich, and A. Harriman, New J. Chem. **31**, 496 (2007).
[28]H. Lu, J. MacK, Y. Yang, and Z. Shen, Chem. Soc. Rev. **43**, 4778 (2014).
[29]G. Ulrich, R. Ziessel, and A. Harriman, Angew. Chem., Int. Ed. **47**, 1184 (2008).
[30]N. Boens, V. Leen, and W. Dehaen, Chem. Soc. Rev. **41**, 1130 (2012).
[31]M. Striccoli, A. Panniello, M. Trapani, M. Cordaro, C. N. Dibenedetto, R. Tommasi, C. Ingrosso, E. Fanizza, R. Grisorio, E. Collini, A. Agostiano, M. L. Curri, and M. A. Castriciano, Chem. – Eur. J. **27**, 2371 (2021).
[32]M. Cordaro, P. Mineo, F. Nastasi, and G. Magazzù, RSC Adv. **4**, 43931 (2014).
[33]L. Bolzonello, A. Polo, A. Volpato, E. Meneghin, M. Cordaro, M. Trapani, M. Fortino, A. Pedone, M. A. Castriciano, and E. Collini, J. Phys. Chem. Lett. **9**, 1079 (2018).
[34]M. Fortino, E. Collini, A. Pedone, and J. Bloino, Phys. Chem. Chem. Phys. **22**, 10981 (2020).
[35]N. Boens, B. Verbelen, M. J. Ortiz, L. Jiao, and W. Dehaen, Coord. Chem. Rev. **399**, 213024 (2019).
[36]E. Cancès, B. Mennucci, and J. Tomasi, J. Chem. Phys. **107**, 3032 (1997).
[37]M. J. Frisch, G. W. Trucks, H. B. Schlegel, G. E. Scuseria, M. A. Robb, J. R. Cheeseman, G. Scalmani, V. Barone, G. A. Petersson, H. Nakatsuji, X. Li, M. Caricato, A. V. Marenich, J. Bloino, B. G. Janesko, R. Gomperts, B. Mennucci, H. P. Hratchian, J. V. Ortiz, A. F. Izmaylov, J. L. Sonnenberg, D. Williams, F. Ding, F. Lipparini, F. Egidi, J. Goings, B. Peng, A. Petrone, T. Henderson, D. Ranasinghe, V. G. Zakrzewski, J. Gao, N. Rega, G. Zheng, W. Liang, M. Hada, M. Ehara, K. Toyota, R. Fukuda, J. Hasegawa, M. Ishida, T. Nakajima, Y. Honda, O. Kitao, H. Nakai, T. Vreven, K. Throssell, J. A. Montgomery, Jr., J. E. Peralta, F. Ogliaro, M. J. Bearpark, J. J. Heyd, E. N. Brothers, K. N. Kudin, V. N. Staroverov, T. a. Keith, R. Kobayashi, J. Normand, K. Raghavachari, A. P. Rendell, J. C. Burant, S. S. Iyengar, J. Tomasi, M. Cossi, J. M. Millam, M. Klene, C. Adamo, R. Cammi, J. W. Ochterski, R. L. Martin, K. Morokuma, O. Farkas, J. B. Foresman, and D. J. Fox, Gaussian 16, Gaussian, Inc., 2016.
[38]T. Yanai, D. P. Tew, and N. C. Handy, Chem. Phys. Lett. **393**, 51 (2004).
[39]L. Wang, I.-S. Tamgho, L. A. Crandall, J. J. Rack, and C. J. Ziegler, Phys. Chem. Chem. Phys. **17**, 2349 (2015).
[40]B. Ventura, G. Marconi, M. Bröring, R. Krüger, and L. Flamigni, New J. Chem. **33**, 428 (2009).
[41]I. P. Pozdnyakov, Y. V. Aksenova, E. G. Ermolina, A. A. Melnikov, R. T. Kuznetsova, V. P. Grivin, V. F. Plyusnin, M. B. Berezin, A. S. Semeikin, and S. V. Chekalin, Chem. Phys. Lett. **585**, 49 (2013).
[42]F. Li, S. I. Yang, Y. Ciringh, J. Seth, C. H. Martin, D. L. Singh, D. Kim, R. R. Birge, D. F. Bocian, D. Holten, and J. S. Lindsey, J. Am. Chem. Soc. **120**, 10001 (1998).
[43]H. L. Kee, C. Kirmaier, L. Yu, P. Thamyongkit, W. J. Youngblood, M. E. Calder, L. Ramos, B. C. Noll, D. F. Bocian, W. R. Scheidt, R. R. Birge, J. S. Lindsey, and D. Holten, J. Phys. Chem. B **109**, 20433 (2005).
[44]E. Collini, Chem. Soc. Rev. **42**, 4932 (2013).
[45]M. Cho, Chem. Rev. **108**, 1331 (2008).
[46]Y. Lee, S. Das, R. M. Malamakal, S. Meloni, D. M. Chenoweth, and J. M. Anna, J. Am. Chem. Soc. **139**, 14733 (2017).
[47]R. Moca, S. R. Meech, and I. A. Heisler, J. Phys. Chem. B **119**, 8623 (2015).
[48]J. D. Hybl, A. Albrecht Ferro, and D. M. Jonas, J. Chem. Phys. **115**, 6606 (2001).
[49]D. B. Turner, R. Dinshaw, K.-K. Lee, M. S. Belsley, K. E. Wilk, P. M. G. Curmi, and G. D. Scholes, Phys. Chem. Chem. Phys. **14**, 4857 (2012).
[50]A. Volpato, L. Bolzonello, E. Meneghin, and E. Collini, Opt. Express **24**, 24773 (2016).
[51]A. Volpato, M. Zerbetto, L. Bolzonello, E. Meneghin, B. Fresch, T. Benelli, L. Giorgini, and E. Collini, J. Phys. Chem. C **123**, 10212 (2019).
[52]A. Olaya-Castro and G. D. Scholes, Int. Rev. Phys. Chem. **30**, 49 (2011).
[53]C. Chudoba, E. T. J. Nibbering, and T. Elsaesser, J. Phys. Chem. A **103**, 5625 (1999).
[54]E. T. J. Nibbering, F. Tschirschwitz, C. Chudoba, and T. Elsaesser, J. Phys. Chem. A **104**, 4236 (2000).
[55]G.-J. Zhao and K.-L. Han, J. Phys. Chem. A **111**, 2469 (2007).
[56]G.-J. Zhao and K.-L. Han, J. Phys. Chem. A **111**, 9218 (2007).
[57]V. Butkus, J. Alster, E. Bašinskaitė, R. Augulis, P. Neuhaus, L. Valkunas, H. L. Anderson, D. Abramavicius, and D. Zigmantas, J. Phys. Chem. Lett. **8**, 2344 (2017).
[58]V. Butkus, D. Zigmantas, D. Abramavicius, and L. Valkunas, Chem. Phys. Lett. **587**, 93 (2013).
[59]V. Butkus, D. Zigmantas, L. Valkunas, and D. Abramavicius, Chem. Phys. Lett. **545**, 40 (2012).
[60]E. Meneghin, C. Leonardo, A. Volpato, L. Bolzonello, and E. Collini, Sci. Rep. **7**, 11389 (2017).
[61]V. M. Huxter, T. A. A. Oliver, D. Budker, and G. R. Fleming, Nat. Phys. **9**, 744 (2013).
[62]T. A. A. Oliver and G. R. Fleming, J. Phys. Chem. B **119**, 11428 (2015).
[63]T. Shimanouchi, *Tables of Molecular Vibrational Frequencies Consolidated Volume I* (National Bureau of Standards, 1972).

[64]M. Righetto, L. Bolzonello, A. Volpato, G. Amoruso, A. Panniello, E. Fanizza, M. Striccoli, and E. Collini, Phys. Chem. Chem. Phys. **20**, 18176 (2018).
[65]D. Green, F. V. A. Camargo, I. A. Heisler, A. G. Dijkstra, and G. A. Jones, J. Phys. Chem. A **122**, 6206 (2018).
[66]E. Meneghin, D. Pedron, and E. Collini, Chem. Phys. **514**, 132 (2018).
[67]L. Lapinski, H. Rostkowska, M. J. Nowak, J. S. Kwiatkowski, and J. Leszczyński, Vib. Spectrosc. **13**, 23 (1996).
[68]T. Fornaro, M. Biczysko, J. Bloino, and V. Barone, Phys. Chem. Chem. Phys. **18**, 8479 (2016).
[69]A. Volpato and E. Collini, Opt. Express **27**, 2975 (2019).
[70]A. Volpato and E. Collini, Opt. Express **23**, 20040 (2015).